Advances in River Sediment Research – Fukuoka et al. (eds)
© 2013 Taylor & Francis Group, London, ISBN 978-1-138-00062-9

Application of steady flows for simulating the local scour depth under time varying flows

T. Esmaeili & T. Sumi
Department of Urban Management, Graduate School of Engineering, Kyoto University, Kyoto, Japan

W.Y. Chang
National Center for High-Performance Computing, Science Based Industrial Park, Hsinchu, Taiwan

A. Vakili
Department of Computer Engineering, Islamic Azad Unversity, Aq Qala Center, Aq Qala, Iran

ABSTRACT: Local scouring in the vicinity of bridge piers which are implemented in the natural streams is the subsequent of 3D complex flow patterns. During the local scour process the accelerated flow develops the local scour depth and if it is not predicted correctly the bridge failure occurs. Local scouring around bridge piers is a strictly time dependent phenomenon and subsequently the evolution of local scour depth under the unsteady flow condition is essential for both structure safety and ecological issues. In the present study, development of local scour depth around a circular pier under time varying flows of the three different types of step-wise hydrographs has been simulated by using a fully 3D numerical program SSIIM along with applying a superposition scheme. Results show good agreement between predicted numerical results and experimental data whereas the error rates of the maximum simulated local scour depths were less than 10%.

1 INTRODUCTION

Due to the diverse economic and social costs that can be imposed by bridge failure the evaluation of the maximum local scour depth around bridge piers is an important topic in river engineering. Streambed scour is the leading cause of bridge failure in the United States (Murillo 1987). The costs associated with restoring damaged structures are substantial, but the indirect costs associated with the disruption of traffic can be more than four times the direct costs (Rhodes & Trent 1999). Implementation of bridges' pier foundation in a deeper depth than the maximum potential local scour hole was accepted as a conservative scour countermeasure in most of practical cases although, that would require expensive and deep piers in the streambeds (Esmaeili et al. 2011).

The three-dimensional flow field around a bridge pier is extremely complex due to separation and generation of multiple vortices. The complexity of the flow field is further compounded by the dynamic interaction between the flow and the moveable boundary during the development of a scour hole (Raudkivi 1986). Local scouring around bridge piers can be a severe problem, especially when a high flow occurs in the river (Esmaeili et al. 2009). When this undesirable event occurs, a scour hole develops around bridge piers as, in general, the local scour depth increases with increasing flow (Dehghani et al. 2012). If the severe scour finally exposes the pier foundation in the scour hole, the safety and stability of the bridge will be in danger. Therefore, there is a great need to develop good prediction methods for pier scour evolution especially under the time varying flows of the flood hydrograph.

Many studies have been carried out to develop the relationships for predicting the maximum local scour depth at bridge piers under clear-water scour and other idealized conditions, such as steady flow, uniform sediment, simplified geometry, etc. Although these relations used extensively for design purposes but, most of them are based on equilibrium condition using the peak flood flow, which are only achieved after a long time period, so that in the realistic cases the peak flood flows usually may not last long enough to develop equilibrium scour depth. Thus, the equilibrium scour depth in clear water may yield considerably greater values of scour depth than may occur if the flow is of shorter duration (Dehghani et al. 2009, Chang et al. 2004). For a known time-to-peak value of design flood hydrograph, smaller scour depths

may be obtained which reduce the total cost of construction (Yanmaz 2006). Figure 1 shows the bridge failure during the time varying flow of a flood event in a rural area with a limited access road network.

Some researchers have focused on the scour-depth evolution with uniform sediment under steady flow condition (e.g. Yanmaz & Altinbilek 1991, Melville & Chiew 1999). Mia & Nago (2003) proposed a method for computing the time variation of local scour depth. Their method considered the development of bed shear stress around the pier according to bed-load sediment transport theory. Kothyari et al. (1992) studied the temporal variation of scour depth around bridge piers under clear-water conditions by using unsteady flow that was approximated by a stepwise discharge hydrograph. Nowadays, modeling 3D flow field and bed deformations is practically feasible because of the considerable reduction in computational time and costs.

A 3D flow model, EllipSys 3D, was developed by Roulund et al. (2005) and coupled with a morphologic model to simulate the scour process around a circular pier in uniform sediment. Nagata et al. (2005) developed a 3D numerical model for simulating the flow and bed deformation around river hydraulic structures such as bridge piers. Recently, the SSIIM program has been used by Bihs and Olsen (2008) and the time scaled scour hole development around a circular pier was simulated.

Moreover, evaluation of changes in river geomorphology (i.e. variation of river bed in the vicinity of river hydraulic structures) caused by various unsteady flow regimes is one of the interests of researchers focusing on river ecology issues. Furthermore, assessing the variation of bed softness and subsequently the habitat structures of aquatic animals as well as dynamic changes of the sandbars geometry as a result of time varying flows are essential for discussing about real time scaled river ecology.

In the present study, the SSIIM program was used to simulate the scour depth evolution around a circular bridge pier by applying the concept of superposition procedure which was introduced by Chang et al. (2004). The SSIIM program, implements fully 3D numerical model developed by Olsen (2011), is based on the finite volume method solving the Navier-Stokes equations with the various turbulence models for 3D flows, and solving sediment continuity equation for bed variations (Olsen et al. 1999). This program was made for using in river/environmental/hydraulic and sedimentation engineering but, the main objective was sediment transportation. The main advantage of SSIIM program compared to other Computational Fluid Dynamics (CFD) programs is simulation of sediment transport with moveable bed in complex geometry.

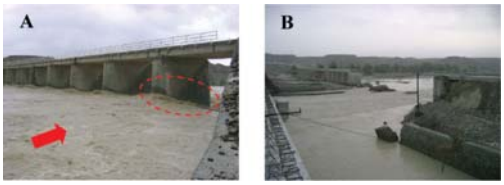

Figure 1. A) Flow pattern in the vicinity of a bridge piers during a flood. B) Failure of the bridge during the flood.

2 NUMERICAL MODEL SSIIM

2.1 *Three dimensional flow model*

The SSIIM program solves the Navier-Stokes equations with the k-ε model on a three dimensional general non-orthogonal coordinates. These equations are discretized with a control volume approach. The SIMPLE or SIMPLEC methods can be used for solving the pressure-poisson equation. An implicit solver is used, producing the velocity field in the computational domain. The velocities are used when solving the convection-diffusion equations for different sediment sizes (Olsen 2011).

The Navier-Stokes equations for non-compressible and constant density flow can be modeled as:

$$\frac{\partial u_i}{\partial x_i} = 0 \tag{1}$$

$$\frac{\partial u_i}{\partial t} + u_j \frac{\partial u_i}{\partial x_j} = \frac{1}{\rho} \frac{\partial}{\partial x_j} \left(-P\delta_{ij} - \rho \overline{u'_i u'_j} \right) \tag{2}$$

where the first term on the left side of the Equation 2 is the transient term. The next term is the convective term. The first term on the right-hand side is the pressure term and the second term on the right side of the equation is the Reynolds stress term. In order to evaluate this term, a turbulence model is required. SSIIM program can use different turbulence models, such as the standard k-ε model or the k-ω model by Wilcox (2000). However, the default turbulence model is the standard k-ε model.

The free surface is modeled as a fixed-lid, with zero gradients for all variables. The locations of the fixed lid and its movement are as a function of time, which can be computed by different algorithms. The 1D backwater computation is the default algorithm and it is invoked automatically. Pressure and Bernoulli algorithm can be used for both steady and unsteady computations. The algo-

rithm is based on the computed pressure field. It uses the Bernoulli equation along the water surface to compute the water surface location based on one fixed point that does not move. The algorithm is fairly stable, so that it can also be used in connection with computation of sediment transport and bed changes (Olsen 2011).

For the wall boundary treatment, it is assumed that the velocity profile follows a certain empirical function called a wall law. It is a semi-analytical function to model the turbulence near the wall in the boundary layer and consequently the CFD model will not need to resolve the turbulence of flow in boundary layer. As a result, it would not necessary too many grid points near the wall:

$$\frac{U}{u_x} = \frac{1}{\kappa}\ln\left(\frac{30y}{k_s}\right) \tag{3}$$

where the shear velocity is denoted u_x, κ is a constant equal to 0.4, y is the distance to the wall and k_s is the roughness equivalent to a diameter of particles on the bed.

2.2 *Morphological model*

The sediment transport process in rivers is described by the following equation, Exner's equation, which is the sediment continuity equation integrated over the water depth:

$$(1-\lambda)\frac{\partial z_b}{\partial t} + \frac{\partial q_{tx}}{\partial x} + \frac{\partial q_{ty}}{\partial y} = 0 \tag{4}$$

where z_b is the bed elevation, λ is the porosity of bed material, and q_{tx} and q_{ty} are components of total-load sediment transport in x- and y-directions, respectively.

In this 3D CFD program, the suspended load can be calculated with the convection-diffusion equation for the sediment concentration, which is expressed as follows:

$$\frac{\partial c}{\partial t} + u_j\frac{\partial c}{\partial x_j} + w\frac{\partial c}{\partial z} = \frac{\partial}{\partial x_j}\left(\Gamma_T\frac{\partial c}{\partial x_j}\right) \tag{5}$$

where w is the fall velocity of sediment particles and Γ_T is the diffusion coefficient and can be expressed in the following way:

$$\Gamma_T = \frac{\nu_T}{Sc} \tag{6}$$

where Sc is the Schmidt number representing the ratio of diffusion coefficient to eddy viscosity coefficient v_t and set to 1.0 as default.

For calculating the suspended load in Equation 4, Equation 5 is solved incorporated with the formula by van Rijn (1987) for computing the equilibrium sediment concentration close to the bed as the bed boundary. In order to solve Equation 4 and Equation 5, conditions of z and C should be given at inflow and outflow boundaries. For the inlet boundary, due to the clear water scour conditions, z = C = 0 can be given and for the outlet boundary, far away from the pier, $\partial C/\partial x = \partial z/\partial x = 0$ can be given due to the uniform flow.

The concentration formula has the following expression:

$$C_{bed} = 0.015\frac{d^{0.3}}{a}\frac{\left[\dfrac{\tau-\tau_c}{\tau_c}\right]^{1.5}}{\left[\dfrac{(\rho_s-\rho_w)g}{\rho_w\nu^2}\right]^{0.1}} \tag{7}$$

where, C_{bed} is the sediment concentration, d is the sediment particle diameter, a is a reference level set equal to the roughness height, τ is the bed shear stress, τ_c is the critical bed shear stress for movement of sediment particles according to Shield's curve, ρ_w and ρ_s are the density of water and sediment, ν is the viscosity of the water and g is the acceleration of gravity.

Once Equation 5 is solved, the suspended load can be calculated as follows:

$$q_{s,i} = \int_a^{z_f} u_i c\ dz \tag{8}$$

where $q_{s,i}$ (i = 1,2) are components of suspended-load sediment transport in x- and y-directions, respectively.

For calculating the bed load in Equation 4, the following relation proposed by van Rijn's formula (1987) is used:

$$\frac{q_b}{D_{50}^{1.5}\sqrt{\dfrac{(\rho_s-\rho_w)g}{\rho_w}}} = 0.053\frac{\left[\dfrac{\tau-\tau_c}{\tau_c}\right]^{1.5}}{D_{50}^{0.3}\left[\left(\dfrac{(\rho_s-\rho_w)g}{\rho_w\nu^2}\right)\right]^{0.1}} \tag{9}$$

where D_{50} is the mean size of sediment. Then, the components of bed-load sediment transport in x- and y-directions can be calculated as follows:

$$q_{bx} = q_b\cos(\alpha_b);\ q_{by} = q_b\sin(\alpha_b) \tag{10}$$

where α_b is the direction of bed-load sediment transportation.

3 MODEL PROPERTIES AND STUDY CASE

The experimental results of Chang et al. (2004) were used for calibration and validation of model. In their study, the experiments were carried out in a 36 m long, 1 m wide and 1.1 m deep flume. A false floor was set in the flume with a recess of 2.8 m long and 0.3 m deep. A hollow cylindrical pier made of transparent plexiglas with a diameter of 0.1 m was located at the center of the recess. The recess was filled with the desired sediment size and was flattened before each experiment run. Chang et al. (2004) & Dehghani et al. (2012) concluded that the recession limb of hydrograph plays much less effective role than rising limb in scour depth evolution. Subsequently, three different stepwise discharge hydrographs were used for simulation of the unsteady flow in channel entrance (Fig. 2).

Figure 2 shows that the hydrographs A, B and C have the same time to peak (t_p) and different peak-flow discharge (Q_p). So, due to the different flow volume, the induced bed shear stress and sediment transport capacity for each of the aforementioned hydrographs will be different.

The boundary condition of discharge and water level during first hour is same for all types of stepwise hydrographs and equal to 0.034 (m^3/s) and 0.15 (m). The temporal variation of the bed surface profile around the pier was recording using two 3 cm long charge coupled device with 2 mm diameter lenses, placed in the hollow plexiglas pier. Uniform sediments were used for unsteady flow condition and the median size of sediment is 0.71 mm with σ_g of 1.2. The experimental results showed that the scour depth increases steadily during the rising period of the hydrograph and the significant amount of final scour depth will be obtained at the end of rising period of hydrograph.

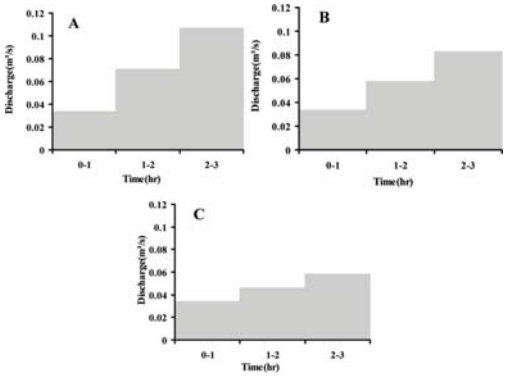

Figure 2. Stepwise discharge hydrographs used for modeling (Chang et al., 2004).

4 NUMERICAL SIMULATIONS

4.1 *Domain description and model calibration*

Making an appropriate grid is a very important process in the preparation of input data for SSIIM program. The size and alignment of the cells will strongly influence the accuracy, the convergence and the computational time (Olsen 2011). For getting more precise results, it is better to refine the mesh around bridge piers (Dehghani et al. 2009). A preprocessing code was used for dividing flow field area into regions of different sizes. In this study, the length of channel is divided by six sections and in each section the various cell sizes were used. The distribution of mesh in half of the channel length is presented in Figure 3.

In the first region, in x- and y-directions, the size of cells is 5 cm × 1 cm and in the second region cells are 2.5 cm × 1 cm. The central part of the flume is 3 m long and the size of cells is 1 cm × 1 cm. The total number of cells in the computational domain is 546000.

For the inflow boundary condition, the velocity distribution was specified while the gradient of pressure is given zero. At the outflow boundary, the vertical gradient of velocity is zero and the hydrostatic pressure distribution is specified according to the water depth. For the solid boundary, wall laws introduced by Schlichting (1979) were used for the side walls and the bed. As previously mentioned, the experimental conditions are the same for the first hour of all stepwise hydrographs. In order to model calibration, by running the SSIIM program, variation of computed scour depth

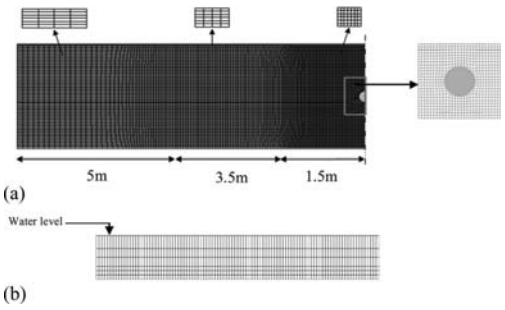

Figure 3. a) Plan view of computational mesh used for numerical modeling (not scale) and b) Corresponding vertical grid distribution.

against time under steady flow condition of first step of stepwise hydrographs was compared with the experimental results and when numerical and experimental results adapted well, then the corresponding time step and roughness were accepted as the calibrated time step and roughness. This process has been illustrated in Figure 4. The time step and roughness were obtained 5 s and 5.2 mm respectively.

Dehghani et al. (2012) found that when the ratio of peak-flow discharge to the discharge of first step increases, the discrepancy between the experimental and numerical model results further magnifies. They also attributed the reason to sharp increase of the side slope of scour hole and in such a condition the scour depth may increase too quickly to cause the side slope of scour hole to exceed the repose angle of sediment in the moveable area around the pier. Moreover, they concluded that numerical program could not respond immediately to the change of discharge as well as boundary condition. So due to the considerable difference between the peak-flow discharge and the discharge of first step, recalibration of the sediment related parameters (i.e. repose angle of sediment as well as bed rouhness) will be necessary in the cases with sharp increase of discharge.

4.2 *Procedure for simulating the scour depth evolution under time varying flows & discussion*

The concept of superposition procedure which introduced by Chang et al. (2004) was used for simulation of scour depth evolution under time varying flows of stepwise hydrographs. As shown in Figure 5b, the scour depth evolves from 0 to S_1 in segment A'B' for Q_0, under the stepwise hydrograph, is in the same way as segment AB along the C_0 curve for steady flow Q_0 shown in Figure 5a. At the end of segment A'B', the scour depth S_1 at time T_A becomes the scour depth at the beginning of the following segment C'D'. In this way, the memory of segment A'B' is brought into segment C'D'. Similarly, for discharge Q_1 of the stepwise hydrograph, the scour-depth evolution along segment C'D' is the same as the corresponding segment CD along C_1 curve for steady flow Q_1. Likewise, the same procedures are applied to the remaining segments of the stepwise hydrograph. In the present study, the curves C_i in Figure 5a for steady flow discharges are obtained by SSIIM program.

After the model calibration, the temporal variation of scour depth around circular bridge pier under boundary condition of each step of stepwise hydrographs has been conducted by employing the SSIIM program. Figure 6 illustrates the scour depth development under each step's boundary condition.

Figure 7 demonstrates the local scour depth evolution under the unsteady flow condition of hydrographs by using the aforementioned superposition procedure. As can be clearly observed

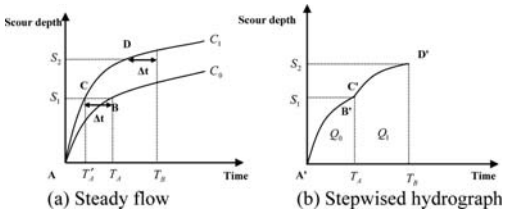

Figure 5. Illustrations of superposition scheme for computing scour depth evolution under stepwise hydrograph.

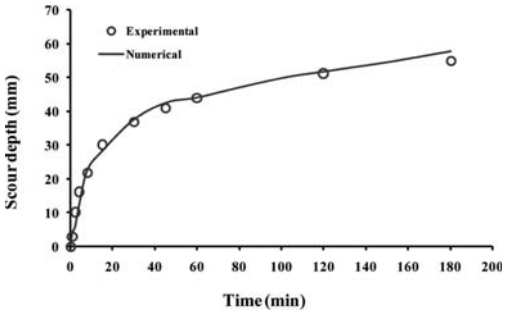

Figure 4. Evolution of local scour depth against time under steady flow condition of first step of stepwise hydrographs for calibrating the model.

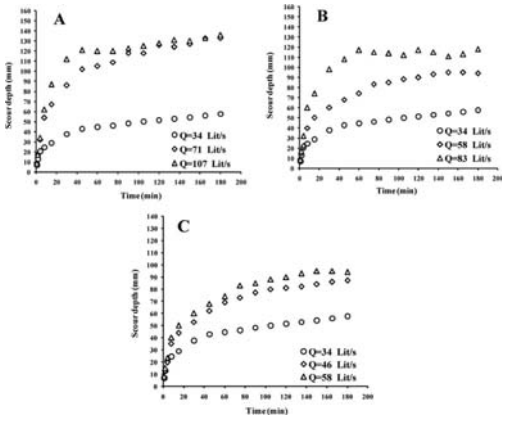

Figure 6. Temporal variation of local scour depth around circular pier under steady flow condition of each step of A) hydrograph A, B) hydrograph B, C) hydrograph C.

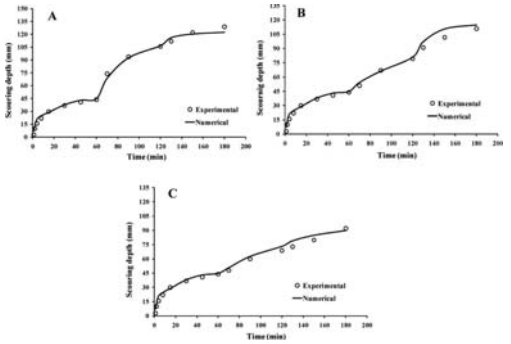

Figure 7. Variation of computed scour depth against time; A) hydrograph A, B) hydrograph B, C) hydrograph C.

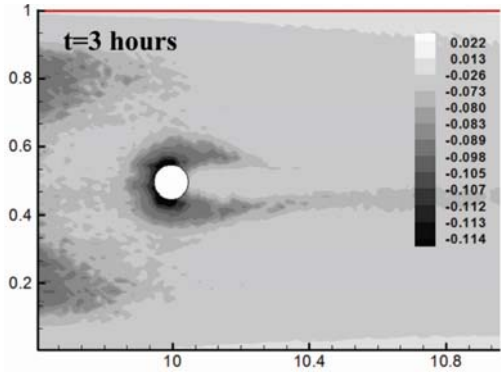

Figure 8. Final bed topography by employing the step-wised boundary condition of hydrograph B.

from Figure 7, there is a good agreement between the experimental and numerical results under the boundary condition of all types of hydrographs.

Furthermore, Results demonstrate that the difference between the maximum simulated local scour depth and measured one at the end of hydrographs A, B and C is less than 10%. So it is concluded that this superposition scheme in connection with numerical model results, as an approach, could provide the accurate results to predict the local scour depth evolution around bridge piers under time varying flows by employing steady flows. The main application of this approach would be designing of temporal bridges with a limited service period or main bridges in transportation networks when the safe and cost-effective designing have a direct relation with the implementation depth of the foundation.

It should be noted that, high peak flow discharges during a flood will have an important role in river geomorphology formation by eroding and depositing of sediments in the main channel stream and flood plains. Prevalent examples about the role of high flow discharge (i.e. floods), in changing the geomorphology of the rivers, are erosion and deposition of sediments in sand bar areas as well as river meanders that strongly influence the habitat structures and subsequently the biodiversity in each river segment. Takemon (1997) derived that development of transition zone in the upper part of a bar structure in a riffle, when sedimentation increases during the floods, may result in increasing the porosity of the substrate and well drainage of underflow water in streams. Also, Reice (1994) concluded that impacts of frequent disturbance in streams such as floods and their effects on creating environmental patches for populations is important for diversity of aquatic species. Though the high flow discharges during the time varying flows have the dominant roles for changing the geometry of whole habitat structures, consequent low flow discharges are able to have a function for initiating the second small scale erosion and deposition in previously scoured or deposited areas. So the second stage grain size redistribution and new bed softness would be considered as the low-flow discharges effects on river geomorphology during the unsteady flows.

As a result, from the eco-hydraulic point of view, it will be useful to simulate the local scour geometry evolution under time varying flows because of their role in eroding and depositing of sediments around the bridge piers which will be a potential habitat for some aquatic animals. Figure 8 shows the bed changes in the vicinity of the circular pier under the boundary condition of the 3rd hour of hydrograph B. This figure clearly demonstrates the local scour geometry and also bed changes pattern around the pier.

5 CONCLUSIONS

In this study the evolution of scour depth was simulated by a 3D numerical program and a superposition scheme was employed for connecting the results of steady flow condition to the time varying flows of 3 different types of hydrographs. The method was based on employing the scour depth evolution under the steady discharge corresponding to each step of the step-wise hydrograph. The following outcomes were obtained from this study:

1. In this study, the superposition concept along with the satisfactory ability of the 3D numerical program SSIIM for providing the accurate scour depth development under steady flows corresponds to the discharge of each step of

stepwised hydrograph is the basis of the connection between the steady flows and time varying flows of hydrographs as an approach. Comparing the simulated results with the experimental data shows good agreement. In this way the complex condition of time varying flows of hydrographs will break into simple case of steady flows. This approach can be useful for safe and cost effective designing of not only bridge piers, but also other river structures (i.e. groynes, abutments) which are periodically exposed to time varying flows of different floods.

2. The result accuracy of the numerical program is tightly depends on the calibration and adjustment of the model. In this study by employing the superposition concept, the error rate of the calculated scour depth at the end of the hydrographs was less than 10%.
3. The Main aspect of the present study is to show that the amount of predicted local scour under unsteady hydrographs is less than the equilibrium local scour depth under a steady flow, which is related to the peak flow discharge. As for the engineering applications for temporal hydraulic structures, the proposed method may be capable of scour assessment in the field situations, in which the hydrographs should be appropriately stepwised beside of considering the type of hydrograph for adjusting the model.
4. Although this superposition scheme could predict the local scour depth under time varying flows of hydrographs, the development of local scouring geometry during the rising period of the hydrograph cannot be provided by this scheme. Owing to the fact that geomorphology changes in main channel stream in where some hydraulic structures are implemented, may affect the habitat structures of some aquatic organisms, it is necessary to have a concept for monitoring the stepwise changes in the bed topography during the unsteady flows for future studies. In this way, it will be possible to monitor the time-scaled topography changes of a designated location in alluvial streams (i.e. in the vicinity of hydraulic structures such as bridge piers or groynes) and considering both the structure safety issues and ecological challenging aspects of hydraulic structures construction in one frame work.

ACKNOWLEDGEMENT

First author would like to give his sincere gratitude to Assoc. Prof. Yasuhiro TAKEMON for his useful comments on the paper.

REFERENCES

Bihs, H. & Olsen, N.R.B. 2008. Three dimensional numerical modeling of pier scour. In H. Sekiguchi (ed.), *4th International conference on scour and erosion; Proc intern. conf., Tokyo, 5–7 November 2008. Tokyo.*

Chang, W.Y. Lai, J.S. & Yen, C.L. 2004. Evolution of scour depth at circular bridge piers. *Journal of Hydraulic Engineering ASCE* 130(9): 905–913.

Dehghani, A.A. Esmaeili, T. Chang, W.Y. & Dehghani, N. 2012. 3D numerical simulation of local scouring under hydrographs. *Proceedings of the Institution of Civil Engineers Journal Water Management* 166(3): 120–131.

Dehghani, A.A. Esmaeili, T. Kharaghani, S. & Pirestani M.R. 2009. Numerical simulation of scour depth evolution around bridge piers under unsteady flow condition. In International Association of Hydraulic Engineering and Research (ed.), *33rd IAHR Congress: Water Engineering for a Sustainable Environment; Proc. intern. conf., Vancouver, 9–14 August 2009. Vancouver.*

Esmaeili, T. Dehghani, A.A. Pirestani, M.R. & Sumi, T. 2011. Numerical simulation of skewed slot effect on local scour reduction. *Journal of Water Sciences Research JWSR* 3(1): 69–80.

Esmaeili, T. Dehghani, A.A. Zahiri A.R. & Suzuki K. 2009. 3D numerical simulation of scouring around bridge piers (casestudy: Bridge 524 crosses the Tanana River). *World Academy of Science and Technology* 58: 1557–1561.

Kothyari, U.C. Garde, R.J. & Range Raju K.G. 1992. Temporal variation of scour around circular bridge piers. *Journal of Hydraulic Engineering, ASCE* 118(8): 1091–1106.

Melville, B.W. & Chiew Y.M. 1999. Time scale for local scour at bridge piers. *Journal of Hydraulic Engineering, ASCE* 125(1): 59–65.

Mia, M.F. & Nago, H. 2003. Design model of time-dependent local scour at circular bridge piers. *Journal of Hydraulic Engineering, ASCE* 130(6): 420–427.

Murillo, J.A. 1987. The scourge scour. *Journal of Hydraulic Engineering, ASCE* 57(7): 66–69.

Nagata, N. Hosoda, T. Nakato, T. & Muramoto Y. 2005. Three dimensional numerical model for flow and bed deformation around river hydraulic structures. *Journal of Hydraulic Engineering, ASCE* 131(12): 1074–1087.

Olsen, N.R.B. 2011. A three dimensional numerical model for simulation of sediment movement in water intakes with multiblock option. Trondheim: SSIIM online user's manual, http://www.ntnu.no.

Olsen, N.R.B. Jimenes, O.F. Abrahamsen L. & Lovoll A. 1999. 3D CFD modeling of water and sediment flow in a hydropower reservoir. *International Journal of Sediment Research* 14(1): 1–8.

Raudkivi, A.J. 1986. Functional trends of scour at bridge piers. *Journal of Hydraulic Engineering, ASCE* 112(1): 1–13.

Reice, S.R. 1994. Nonequilibrium determinants of biological community structures. *American Scientists,* 82(5): 424–435.

Rhodes, J. & Trent, R.E. 1999. Economic of floods, scour and bridge failures. In Richardson, E.V. & Lagasse P.F. (ed.), *Stream stability and scour at highway bridges; Proc. intern. conf., San Francisco, California, 25–30 July 1993.* Reston, Virginia: ASCE.

Roulund, A. Sumer, B.M. Fredsoe, J. & Michelsen, J. 2005. Numerical and experimental investigation of flow and scour around a circular pile. *Journal of Fluid Mechanics* 534: 351–401.
Schlichting, H. 1979. *Boundary-Layer Theory.* New York: Mc-Graw Hill.
Takemon, Y. 1997. T. Abe, S. Levin & M. Higashi (eds), *Biodiversity: An ecological prospective:* 259–275. New York: Springer-Verlag.
Wilcox, D.C. 2000. *Turbulence modeling for CFD.* California: DCW Industries Inc.
Yanmaz, A.M. 2006. Temporal variation of clear water scour at cylindrical bridge piers. *Canadian Journal of Civil Engineering* 33(8): 1098–1102.